
AFRL-RZ-WP-TP-2010-2115

# CFD PREDICTIONS OF PULSED FILM COOLING HEAT FLUX ON A TURBINE BLADE LEADING EDGE (Postprint)

**Richard Rivir**

**Turbine Branch**
**Turbine Engine Division**

**James L. Rutledge and Paul I. King**

**Air Force Institute of Technology**

**APRIL 2010**
**Interim Report**



**AIR FORCE RESEARCH LABORATORY**
**PROPULSION DIRECTORATE**
**WRIGHT-PATTERSON AIR FORCE BASE, OH 45433-7251**
**AIR FORCE MATERIEL COMMAND**
**UNITED STATES AIR FORCE**

# REPORT DOCUMENTATION PAGE

*Form Approved*
*OMB No. 0704-0188*



| 1. REPORT DATE *(DD-MM-YY)* | 2. REPORT TYPE | 3. DATES COVERED *(From - To)* |
|---|---|---|
| April 2010 | Journal Article Postprint | 01 April 2010 – 01 April 2010 |

**4. TITLE AND SUBTITLE**
CFD PREDICTIONS OF PULSED FILM COOLING HEAT FLUX ON A TURBINE BLADE LEADING EDGE (Postprint)

**5a. CONTRACT NUMBER**
IN HOUSE

**5b. GRANT NUMBER**

**5c. PROGRAM ELEMENT NUMBER**
61102F

**6. AUTHOR(S)**
Richard Rivir (Turbine Engine Division, Turbine Branch (AFRL/RZTT))
James L. Rutledge and Paul I. King (Air Force Institute of Technology)

**5d. PROJECT NUMBER**
2307

**5e. TASK NUMBER**
06

**5f. WORK UNIT NUMBER**
2307S314

**7. PERFORMING ORGANIZATION NAME(S) AND ADDRESS(ES)**

Turbine Branch (AFRL/RZTT)
Turbine Engine Division,
Air Force Research Laboratory, Propulsion Directorate
Wright-Patterson Air Force Base, OH 45433-7251
Air Force Materiel Command
United States Air Force

Air Force Institute of Technology

**8. PERFORMING ORGANIZATION REPORT NUMBER**
AFRL-RZ-WP-TP-2010-2115

**9. SPONSORING/MONITORING AGENCY NAME(S) AND ADDRESS(ES)**

Air Force Research Laboratory
Propulsion Directorate
Wright-Patterson Air Force Base, OH 45433-7251
Air Force Materiel Command
United States Air Force

**10. SPONSORING/MONITORING AGENCY ACRONYM(S)**
AFRL/RZTT

**11. SPONSORING/MONITORING AGENCY REPORT NUMBER(S)**
AFRL-RZ-WP-TP-2009-2115

**12. DISTRIBUTION/AVAILABILITY STATEMENT**
Approved for public release; distribution unlimited.

**13. SUPPLEMENTARY NOTES**
PAO Case Number: AFIT/JA-080252; Clearance Date: 20 May 2008. The U.S. Government is joint author of the work and has the right to use, modify, reproduce, release, perform, display, or disclose the work. Published in ASME IMECE 2008 (IMECE2008-67276). Paper contains color.

**14. ABSTRACT**
A computational study was conducted to determine how leading edge film cooling performance is affected by pulsing the coolant flow. Time resolved adiabatic effectiveness and heat transfer coefficient are used to calculate the temporally averaged, spatially resolved net heat flux reduction for several pulsing scenarios. Net heat flux is generally increased by pulsing the film coolant, with greater degradation for higher pulsation amplitudes relative to the average blowing ratio.

**15. SUBJECT TERMS**
Turbine, heat transfer, film cooling, computational modeling

| 16. SECURITY CLASSIFICATION OF: | | | 17. LIMITATION OF ABSTRACT: | 18. NUMBER OF PAGES | 19a. NAME OF RESPONSIBLE PERSON (Monitor) |
|---|---|---|---|---|---|
| a. REPORT | b. ABSTRACT | c. THIS PAGE | | | Rolf Sondergaard |
| Unclassified | Unclassified | Unclassified | SAR | 16 | 19b. TELEPHONE NUMBER *(Include Area Code)* N/A |

**Standard Form 298 (Rev. 8-98)**
Prescribed by ANSI Std. Z39-18

**Proceedings of IMECE2008**
**2008 ASME International Mechanical Engineering Congress and Exposition**
**October 31-November 6, 2008, Boston, Massachusetts, USA**

# IMECE2008-67276

# CFD PREDICTIONS OF PULSED FILM COOLING HEAT FLUX ON A TURBINE BLADE LEADING EDGE

**James L. Rutledge**
Air Force Institute of Technology
Wright-Patterson AFB, Ohio, USA

**Paul I. King**
Air Force Institute of Technology
Wright-Patterson AFB, Ohio, USA

**Richard Rivir**
Air Force Research Laboratory
Wright-Patterson AFB, Ohio,
USA

## ABSTRACT

*Unsteadiness in film cooling jets may arise due to inherent unsteadiness of the blade-vane interaction or may be induced as a means of flow control. A computational study was conducted to determine how leading edge film cooling performance is affected by pulsing the coolant flow. A cylindrical leading edge with a flat afterbody is used to simulate the turbine blade leading edge region. A single coolant hole was located 21.5° from the leading edge, angled 20° to the surface and 90° from the streamwise direction. The leading edge diameter to hole diameter ratio is D/d = 18.7. Time resolved adiabatic effectiveness and heat transfer coefficient are used to calculate the temporally averaged, spatially resolved net heat flux reduction for several pulsing scenarios. The net heat flux reduction with pulsed film cooling is compared to the steady jet with matched average mass flow rate. Steady blowing ratios of M = 0.25 and 0.50 are each compared with two pulsed jet cases with matching averaging blowing ratio, $\overline{M}$ , at a nondimensional frequency, F = 0.151 and duty cycle, DC = 50%. Simulations were performed at $Re_D$ = 60000. Net heat flux is generally increased by pulsing the film coolant, with greater degradation for higher pulsation amplitudes relative to the average blowing ratio.*

## NOMENCLATURE

| | | |
|---|---|---|
| $d$ | = | hole diameter (m) |
| $D$ | = | leading edge diameter (m) |
| $DC$ | = | duty cycle (% of time at high $M$) |
| $f$ | = | frequency (Hz) |
| $F$ | = | nondimensional frequency $fD/U_\infty$ |
| $h$ | = | convective heat transfer coefficient, (W / (m$^2$ K)) |
| $L$ | = | length of film cooling hole (m) |
| $M$ | = | blowing ratio, $\rho_c U_c / \rho_\infty U_\infty$ |
| $q''$ | = | convective heat flux into a surface (W / m$^2$) |
| $t$ | = | time (s) |
| $T$ | = | temperature, K or nondimensional time, $tU_\infty / D$ |
| $U$ | = | velocity (m/s) |
| $x$ | = | surface distance downstream of hole centerline (m) |
| $y$ | = | spanwise distance from hole centerline (m) |
| $z$ | = | distance normal to surface into fluid (m) |
| $\Delta q_r$ | = | net heat flux reduction |
| $\eta$ | = | adiabatic effectiveness, $(T_\infty - T_{aw}) / (T_\infty - T_c)$ |
| $\phi$ | = | overall effectiveness, $(T_\infty - T_s) / (T_\infty - T_c)$ |
| $\Lambda$ | = | turbulence integral length scale, m |
| $\theta$ | = | nondimensional temperature, $(T_\infty - T) / (T_\infty - T_c)$ |
| $\rho$ | = | density (kg / m$^3$) |

*Subscripts*

| | | |
|---|---|---|
| 0 | = | without film cooling |
| *aw* | = | adiabatic wall |
| *c* | = | coolant |
| *f* | = | with film cooling |
| *s* | = | surface |
| *span* | = | spanwise averaged |

$\infty$ = mainstream recovery

*Superscripts*

$\bar{}$ = temporal average

' = zero mean fluctuating component

## INTRODUCTION

Film cooling is used in gas turbine engines to protect hot gas path components through the reduction of adiabatic wall temperature. The adiabatic effectiveness is defined as

$$\eta \equiv \frac{T_\infty - T_{aw}}{T_\infty - T_c} \quad \textbf{(1)}$$

and describes the temperature distribution that would occur with no heat transfer. The convective heat flux is related to the adiabatic wall temperature through the heat transfer coefficient given by:

$$h_f = \frac{q_f{}''}{T_s - T_{aw}} \quad \textbf{(2)}$$

In addition to reducing the adiabatic wall temperature below the mainstream recovery temperature, film cooling can influence the heat transfer coefficient; therefore, both parameters must be measured in order to characterize the influence of a film cooling design on the net heat flux. The net heat flux reduction due to film cooling is frequently expressed by the following equation:

$$\Delta q_r = 1 - \frac{h_f}{h_0}\left(1 - \frac{\eta}{\phi}\right) \quad \textbf{(3)}$$

Rutledge et al. [1] demonstrated that simple substitution of the time averaged values of $h_f$ and $\eta$ into Eq. (3) will not account for the cross coupling between the terms to determine the average net heat flux reduction. Instead, a generalized form must be used:

$$\overline{\Delta q_r} = 1 - \frac{\overline{h_f}}{h_0}\left(1 - \frac{\bar{\eta}}{\phi}\right) + \frac{\overline{h_f{}'\eta'}}{h_0\phi} \quad \textbf{(4)}$$

where we use the notation in which a time dependent parameter is written as the sum of a temporal mean and a zero-mean fluctuating component:

$$h(t) = \bar{h} + h'(t) \quad \textbf{(5)}$$

and

$$\eta(t) = \bar{\eta} + \eta'(t) \quad \textbf{(6)}$$

With unsteady computational simulations, determination of time resolved $h_f$ and $\eta$ is simply a matter of outputting the desired data at each time step; therefore, $\overline{\Delta q_r}$ may alternatively be determined by computing Eq. (3) at each time step and taking the temporal average of the quantity. Physical experiments generally rely on average values in which case accurate determination of $\overline{\Delta q_r}$ requires measurement of the cross coupling term found in Eq. (4). The data presented here show the magnitude of this term.

## BACKGROUND

Recent interest in pulsed film cooling has led to several experimental studies of the behavior of pulsed film cooling jets. Ekkad et al. [2] studied the effects of jet pulsation and duty cycle on film cooling from a single jet on a leading edge model. Heat transfer coefficient distributions and adiabatic effectiveness distributions were determined simultaneously through the use of a transient experiment. In their experiment, the model is soaked at an initial temperature $T_i$ prior to the simultaneous nearly instantaneous startup of both the coolant flow and the mainstream flow. Temperatures are selected such that the initial model temperature, coolant temperature and mainstream temperature all differ. By measuring the wall temperature at any two moments in time after test initiation, but prior to thermal wave penetration through the model walls, the heat equation can be solved simultaneously for average $h$ and $T_{aw}$. The researchers found that pulsing a jet at a particular blowing ratio tends to increase the adiabatic effectiveness compared to a steady jet at the same blowing ratio, but the effect on heat transfer coefficient was small. Results were independent of pulsing frequency for all three pulsing frequencies studied which were all $F << 1$. When compared to a steady jet at the same average blowing ratio, some pulsed jets were found to have higher adiabatic effectiveness, but at the cost of higher heat transfer coefficient. This effect was most notable at an average blowing ratio of $\overline{M} = 0.5$, for which pulsing increased the spanwise averaged adiabatic effectiveness between 0.03 and 0.05, with the greater gains farther from the film cooling hole. Similar results occurred with the $M = 1$ jet pulsed at $DC = 50\%$ compared to the steady $M = 1.0$ jet since spanwise averaged adiabatic effectiveness for steady jets at $M = 0.5$ and $M = 1$ happen to be nearly identical. Pulsing increased the heat transfer coefficient by approximately 20% compared to the continuous coolant flow at the same average blowing ratio of $\overline{M} = 0.5$.

Coulthard et al. [3, 4] studied the effects of jet pulsing on film cooling effectiveness and heat transfer coefficient on a flat plate. The researchers used a single row of five holes spaced $3D$ apart, inclined 35° to the surface and parallel to the streamwise direction. Adiabatic effectiveness and heat transfer coefficients were measured in separate experiments. An electrical heat flux plate was used to generate a uniform heat flux, with a separate heat flux plate upstream of the row of coolant holes to develop a thermal boundary layer upstream of the coolant holes. Pulsing the coolant was found to decrease adiabatic effectiveness compared to a steady jet, whether one made the comparison to a steady jet with the blowing ratio

equal to the "on" value of the pulsed jet or a steady jet with the time averaged blowing ratio of the unsteady jet. The researchers observed that pulsing the coolant jets induced a high startup velocity prior to the jet reaching steady state. This high startup velocity may have been responsible for increased jet lift-off with the pulsed jet. The heat transfer coefficient was increased for a pulsed jet compared to a steady jet with the blowing ratio equal to the "on" value of the pulsed jet. However, when compared to a steady jet with the time-averaged blowing ratio of the pulsed jet, the heat transfer coefficient was not necessarily higher than with the steady jet. At the highest pulsing frequencies, the heat transfer coefficient was higher than the steady jet, but as pulsing frequency was decreased, the heat transfer coefficient dropped lower than with the steady jet. At the lowest studied frequency and a duty cycle of $DC = 50\%$, the heat transfer coefficient ratio, $h_f / h_0$, was about 25% lower than with a steady jet with the same average blowing ratio of $M = 0.25$. The general lack of benefit from pulsed film cooling observed in this study might suggest that the effect of pulsing is strongly dependent on the component geometry.

Muldoon and Acharya [5] performed a direct numerical simulation (DNS) of a pulsed coolant jet on a flat plate. The coolant jet was cylindrical, aligned in the streamwise direction and inclined at 35° relative to the plate. The flow was assumed to be incompressible; furthermore, the density of the coolant was assumed to be the same as the freestream. The authors chose to use a domain that did not include the coolant hole. Instead, the elliptic hole exit was set as a boundary condition. This boundary condition used a temporally averaged velocity profile obtained from a separate experiment in which the blowing ratio $M = 1.5$ was simulated. The velocity profiles used for blowing ratios other than $M = 1.5$ were obtained via scaling the $M = 1.5$ velocity profile. A steady jet at $M = 1.5$ was found to contain large scale turbulent structures of approximately the same size as the hole diameter beginning at about $x/d = 4$. These structures also happen to be of a scale that is nearly equal to the distance that the jet resides above the surface for this highly separated jet; therefore, these unsteady structures may play a very important role in the time averaged adiabatic effectiveness. The simulation suggested that strong horseshoe vortices entrain coolant and are beneficial for adiabatic effectiveness. Pulsing the coolant between $M = 1.5$ and $M = 0$ was found to generally improve adiabatic effectiveness compared to the steady jet at $M = 1.5$. On the other hand, pulsing was found to be detrimental to adiabatic effectiveness compared to the steady jet with the average blowing ratio of the pulsed jet. Pulsing was generally found to destroy the beneficial horseshoe vortex detected with the simulations of the steady jet, but downward vortex induction of the starting vortex was found to cause the coolant to reattach.

## COMPUTATIONAL MODEL

A computational model was designed to replicate the geometry used by Ekkad et al. [2]. A single coolant hole of dimension $D/d = 18.7$ in the middle of the computational model has a length to diameter ratio of $L/d = 11.69$, typical of an actual blade. The span of the leading edge is 209 $d$; symmetry boundary conditions are applied at the ends of the span. The computational domain extends 146 $d$ upstream of the leading edge and 146 $d$ above the flat afterbody. Only half of the half-cylinder leading edge is modeled as shown in Fig. 1; the plane defined by extending the stagnation line upstream is modeled as a symmetry boundary condition. The coolant hole inlet boundary condition is set at a plane normal to the axis of the hole with mass flow in the direction of the hole axis distributed uniformly across the surface area of the inlet. The plenum was not modeled due to the high $L/d$ of the coolant hole. Although Leylek and Zerkle [6] conclude there is an influence of the plenum on the coolant hole exit velocity profile, they used a maximum $L/d$ of 3.5, which is only 30% of that used in the present study so the plenum should not have as great an influence in the current study.

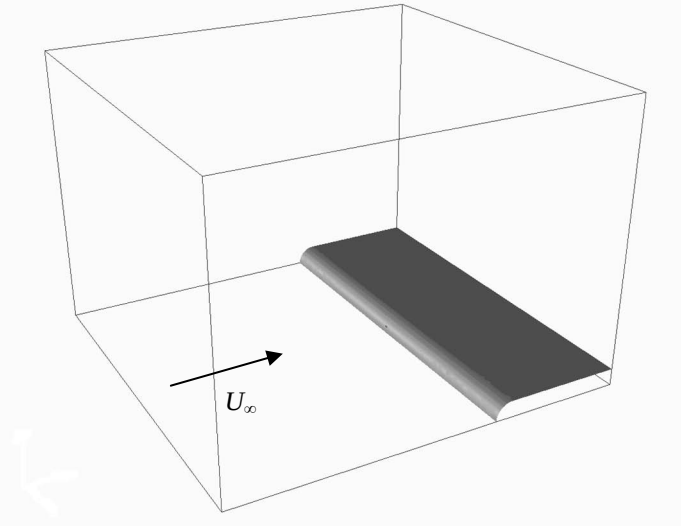


**Fig. 1 Computational Domain**

An unstructured mesh was generated on the computational surfaces using GridGen's implementation of Delaunay triangulation [7]. In order to control the volume grid growth rate away from wall grids, additional "transparent" surface grids (surface grids through which fluid flow is unimpeded in any way) were placed offset from the leading edge and the afterbody a distance of approximately the leading edge radius. The unstructured volume grid was generated using SolidMesh, which uses the Advancing-Front/Local-Reconnection grid generation routine [8]. A prismatic boundary layer growth was used from the wall surfaces to resolve turbulent boundary layers with the nearest cell spaced with $z^+$ of order unity.

In the current study, turbulence is modeled using the realizable $k$-ε model with enhanced wall treatment, which uses a two layer model such that the domain is divided into fully turbulent and viscosity-affected regions [9]. The realizable $k$-ε model has been proven to be superior to the standard $k$-ε model with jets and mixing layers [9] and has been used with some success with steady film cooling flows (e.g., [10]). The turbulence at the pressure inlet and outlet of the computational domain was modeled to have an intensity of $Tu = 1\%$ and a length scale of $\Lambda / d = 2.1$. The coolant hole inlet boundary condition was modeled to have a turbulence intensity of $Tu = 1\%$ and a length scale of $\Lambda / d = 0.42$. Although these turbulence characteristics are atypical of actual engine conditions, they are more representative of the turbulence characteristics of the wind tunnel used by Ekkad et al. [2].

The computational model assumed constant density flow. Fluent's three dimensional node-based segregated solver was used for all computations. All discretization schemes were second order.

Two separate simulations were run in this study—one to determine adiabatic effectiveness and the other to determine heat transfer coefficient. All simulations were performed with a freestream Reynolds number of $Re_D = 60000$. Adiabatic effectiveness was determined by setting the coolant to a temperature different from the freestream temperature with an adiabatic boundary condition on the leading edge surface and measuring the resulting temperature distribution. Adiabatic effectiveness was computed through direct application of Eq. (1), noting that the surface temperature is, by definition, the adiabatic wall temperature since the wall boundary conditions were set to be adiabatic. The heat transfer coefficient was determined by using a coolant temperature equal to the freestream temperature and setting a known heat flux boundary condition on the leading edge surface and measuring the resulting temperature distribution. The surface temperature is related to the heat transfer coefficient through Eq. (2), noting that the adiabatic wall temperature is the freestream temperature since the coolant and freestream temperatures are the same. Net heat flux reduction was calculated using Eq. (4) and a presumed overall effectiveness, $\phi = 0.6$ based on expected values in the literature [11].

## GRID AND TIME STEP CONVERGENCE

In order to establish grid convergence, the steady solver available with Fluent was used and iterative convergence was assumed when the largest scaled residual (usually on ε) was of order $10^{-5}$. When feasible, largest residuals of order $10^{-7}$ were attained. In order to develop a sufficiently fine grid such that the results are grid independent, different sized grids were tested at a steady blowing ratio of $M = 1$. When spanwise averaged across the bulk of the jet ($-2.5 < y / d < 1.5$), the adiabatic effectiveness determined with the 9.2 million cell grid was within 0.5% of the value with the 8.9 million cell grid and within 1.5% of the value with the 7.6 million cell grid. A 9.2 million cell grid was sufficient for grid independence.

In order to resolve a turbulent boundary layer, the first grid point off the wall is at a distance of $z^+$ order unity. Two renderings of the final grid are shown in Figs. 2 and 3. The maximum "wall $z^+$" was determined to be 2.67 along a small part of the intersection of the coolant hole with the outer radius of the leading edge where a sharp edge exists. Aside from this sharp edge, the wall $z^+$ was approximately unity or less than 1.0 with the exception of a region approximately 1$d$ downstream of the fore side of the coolant hole where the wall $z^+$ had a maximum of approximately 1.8. This wall $z^+$ distribution is deemed sufficient since where wall $z^+ > 1.0$, it is still well within the viscous sublayer, that is, wall $z^+ < 5$.

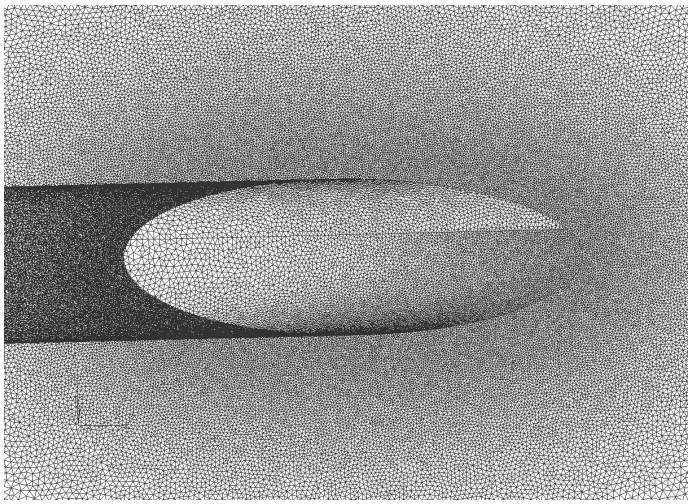

**Fig. 2 Surface mesh on leading edge in vicinity of coolant hole**

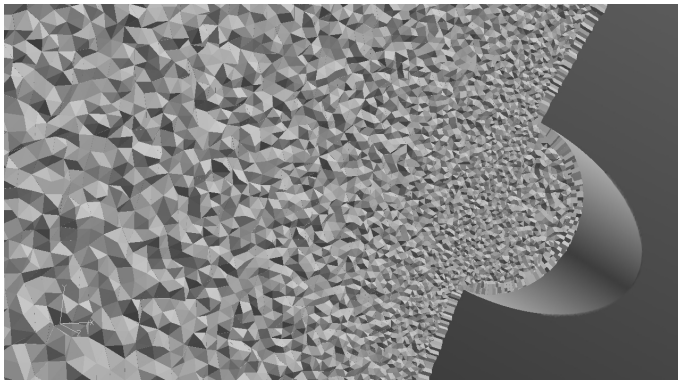

**Fig. 3 Fluid region mesh on streamwise plane bisecting intersection of the coolant hole with the leading edge**

A second order implicit unsteady formulation was used for all unsteady simulations. An iterative time advancement scheme was employed that solved all equations iteratively at each time step. All scaled residuals were driven down to a

maximum of $10^{-6}$ before the solution was considered to be converged for a particular time step.

Time step convergence was established by considering the temporal variation in adiabatic effectiveness at several points on the leading edge whose temperature is significantly influenced by the film cooling hole. Unsteady simulations were performed for $\overline{M} = 0.5$, $F = 0.151$, $DC$ = 50%. The blowing ratio alternated between "on" at $M = 1$ and "off" at $M = 0$ with the blowing "on" for half of the time and the cycle period is $\Delta T = 6.62$. An unsteady simulation was started using the steady-state $M = 1$ results obtained in the process of establishing grid convergence. At $T = 0$ the blowing ratio was set to $M = 0$. At $T = 3.31$, the coolant was turned back on. The cycle was repeated several times in order to establish periodic steady state. It was found that periodic steady state conditions occurred immediately due to $F << 1$, and thus the steady-state results for $M = 1$ were used as the initial conditions for the unsteady simulation. The reason for the convenience will be explained further when the pulsed jet results are discussed.

A time step as low as $\Delta T = 2.65 \times 10^{-4}$ was required for the solution to be sufficiently independent of time step. The step change in the boundary condition at the inlet of the film cooling hole is quite likely to be responsible for the requirement of such a small time step.

## STEADY JET RESULTS

Adiabatic effectiveness contours for the steady $M = 0.50$ jet are shown in Fig. 4. The axis of the hole is such that the coolant has velocity components in the positive $z$ direction and the negative $y$ direction. The freestream flow causes the coolant to turn in the positive $x$ direction. The adiabatic effectiveness contours are similar in streamwise length to the experimental results of Roland [12], although the experimental data show higher adiabatic effectiveness by about $\Delta\eta \approx 0.05$ past $x/d \approx 0.8$. Additional experimental validation is under way. Heat transfer coefficient ratio, $h_f / h_0$, and net heat flux reduction, $\Delta q_r$, are shown in Figs. 5 and 6, respectively. For the purpose of determining the heat transfer coefficient ratio, $h_0$ was determined using the same leading edge cooling hole geometry, but with $M = 0$. A classic fork-tine like pattern in the heat transfer coefficient ratio is evident downstream of the coolant hole. (The fork tines refer to the two regions of elevated heat transfer coefficient extending downstream of the hole) In Fig. 4, the region of elevated adiabatic effectiveness is biased toward the leeward (lower region in the figure) end of the coolant hole; thus, in Fig. 5 the top tine of elevated heat transfer coefficient, where the adiabatic effectiveness was not as high, causes a region of negative net heat flux reduction, i.e. a net heat flux increase, as seen in Fig. 6. In Fig. 5 a small region immediately upstream of the hole as the boundary layer approaches the jet and extending on the leeward side of the hole experiences a decrease in heat transfer coefficient due to film cooling.

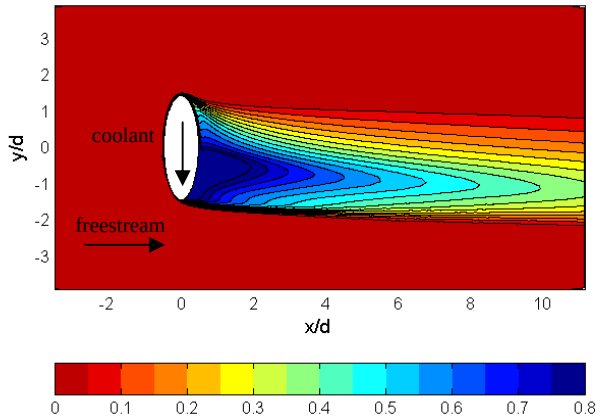


**Fig. 4 Steady $M$ = 0.50 adiabatic effectiveness, $\eta$ (arrows indicate direction of coolant and freestream)**

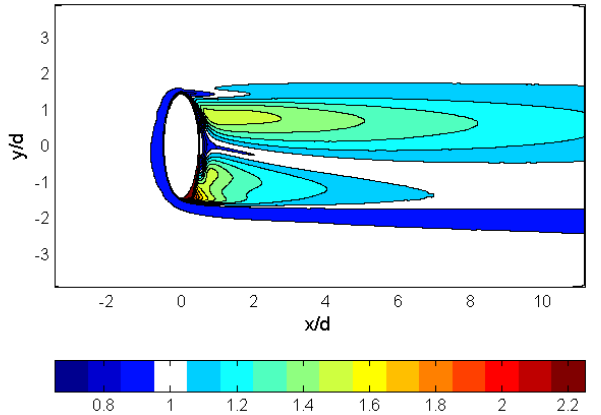


**Fig. 5 Steady $M$ = 0.50 heat transfer coefficient ratio, $h_f / h_0$**

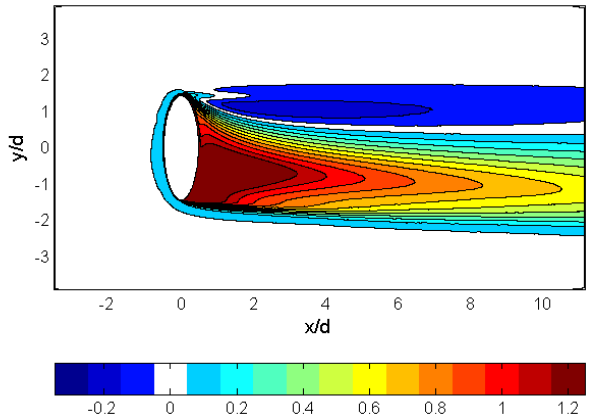


**Fig. 6 Steady $M$ = 0.50 net heat flux reduction, $\Delta q_r$**

Adiabatic effectiveness, heat transfer coefficient ratio, and net heat flux reduction results for the steady $M = 0.25$ jet are shown in Figs. 7, 8, and 9, respectively. Since the $M = 0.25$ jet has a lower momentum flux relative to the freestream, the coolant turns in the direction of the freestream faster than the higher momentum jet and with less lift-off. Thus a region of sufficiently high adiabatic effectiveness coincides with the top tine of elevated heat transfer coefficient to offset that elevation so that that net heat flux reduction is positive everywhere. Furthermore, the lower tine of elevated heat transfer coefficient is much weaker in the $M = 0.25$ case than with the $M = 0.50$ case—so much so that it is nearly indistinguishable as an individual tine.

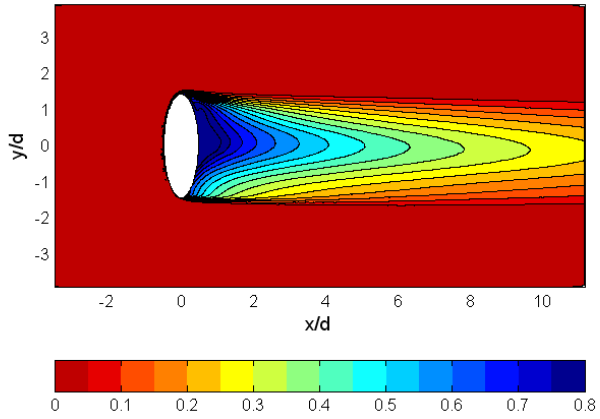


**Fig. 7 Steady $M = 0.25$ adiabatic effectiveness, $\eta$**

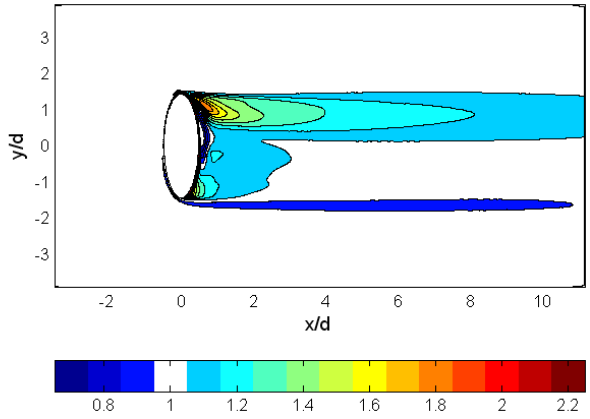


**Fig. 8 Steady $M = 0.25$ heat transfer coefficient ratio, $h_f / h_0$**

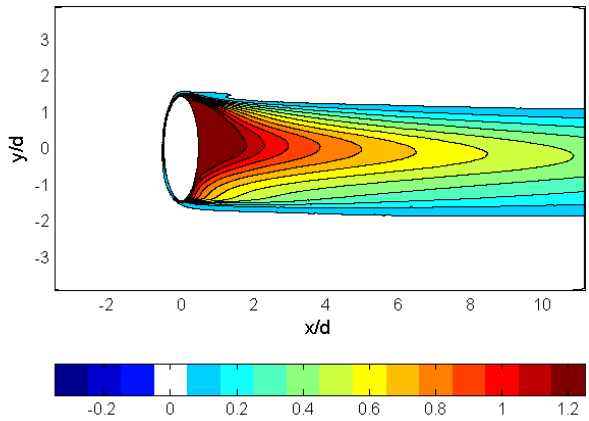


**Fig. 9 Steady $M = 0.25$ net heat flux reduction, $\Delta q_r$**

## PULSED JET RESULTS

All pulsed jet cases are for a nondimensional frequency, $F = 0.151$ and duty cycle, $DC = 50\%$ in a square wave. In actual engine conditions, this nondimensional frequency would correspond to a dimensional frequency in the vicinity of 3500 Hz. The pulsed cases differ from each other only in the minimum and maximum blowing ratios, each with $\overline{M} = 0.5$ or $\overline{M} = 0.25$.

Figure 10 shows adiabatic effectiveness histories for the points shown in Fig. 11 for the case in which the blowing is pulsed between $M = 1$ and $M = 0$ ($\overline{M} = 0.5$). The transient events took place over only approximately one unit of nondimensional time (less than a fifth of the time that the coolant is turned "off"). Indeed, transient events of order one unit of nondimensional time would be expected since it takes one unit of nondimensional time for the freestream to travel one leading edge diameter. Likewise, it takes a discernable amount of time for the adiabatic effectiveness to respond to the step change in blowing ratio, with longer amounts of time required farther downstream from the coolant hole. Perhaps the most striking result is the 27% overshoot in the adiabatic effectiveness at Point F over the steady state value for a short period of time after turning on the coolant (at $T \approx 4.3$). Similar overshoots occur at other points as well.

From Fig. 10, it is evident that the frequency is low enough that the film cooling jet is "on" long enough for steady-state to be attained, i.e., the state of the flow in the region of the cylindrical leading edge at $T = 6.62$ is identical to that which it would be if steady film cooling were used. This aspect of the flow caused periodic steady state to be attained for the very first cycle, provided the initial condition was the steady jet flowfield, as indicated earlier.

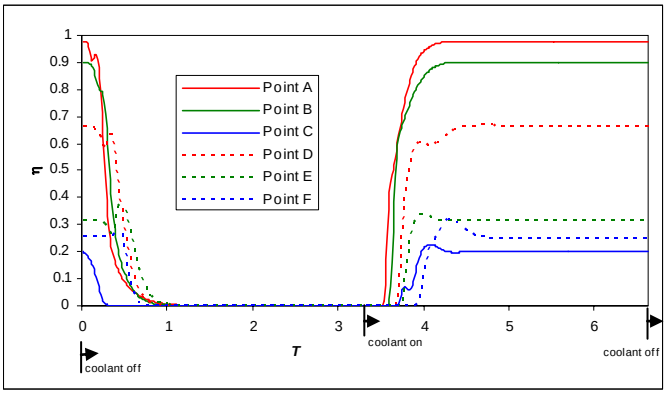


**Fig. 10 Temporally resolved adiabatic effectiveness for several points on leading edge**

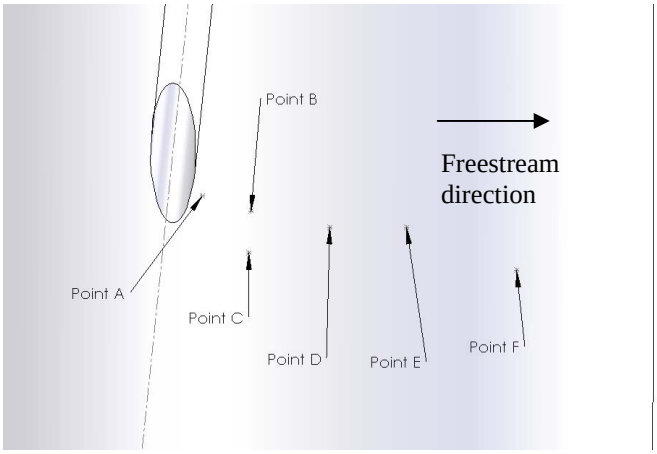


**Fig. 11 Several Points on Leading Edge Surface**

In order to investigate jet lift-off during the steady-state transient start-up event, Fig. 12 shows nondimensional temperature contours for the transient startup event for the case of pulsed coolant between $M = 1$ and $M = 0$ for fluid in a plane normal to the surface at $x/d = 1$. The time period $3.4 \le T \le 4.1$ was selected based on the time period over which the transient event occurs in the near hole region (Points A, B, and C) from Fig. 10. The blowing ratio switches from $M = 0$ to $M = 1$ at $T = 3.31$. By $T = 4.1$, the temperature profile at $x/d = 1$ has nearly reached steady state and there is little change during the interval $4.1 \le T \le 6.6$. At $T = 3.5$ the coolant penetrates the freestream beyond 1 $d$ from the surface at $x/d = 1$ before it settles. Note in Fig. 12, $T = 4.1$, as the contours at $x/d = 1$ have reached steady-state, the coolest region of fluid at $y/d = 0$ is separated from the surface by a third of a hole diameter. This jet lift-off is indicative of inefficient use of coolant at $M = 1$.

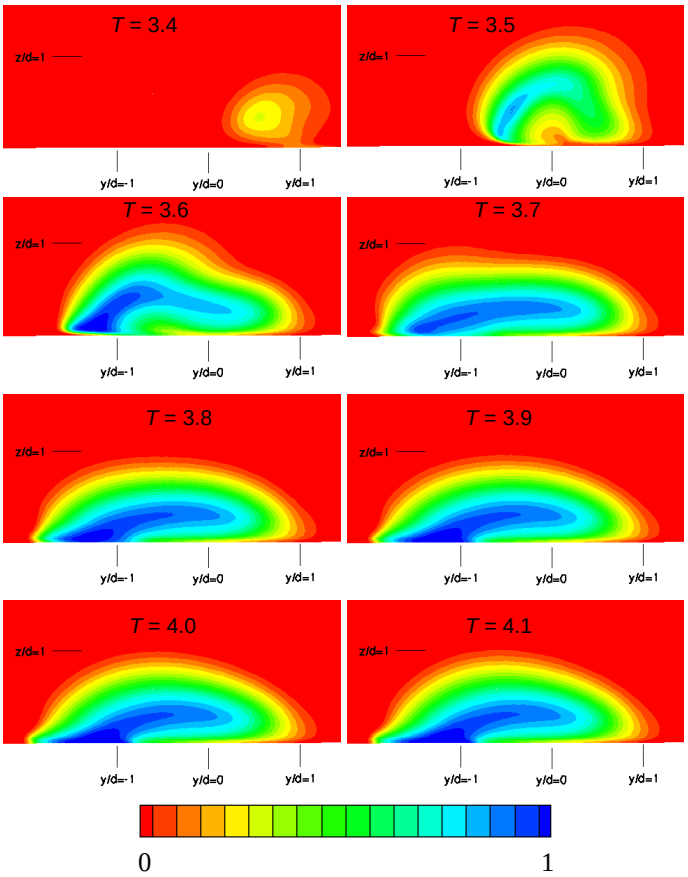


**Fig. 12 Nondimensional temperature distribution, $\theta$, for fluid in plane intersecting surface at $x/d = 1$ for transient jet startup for the case of pulsed coolant between $M = 1$ and $M = 0$, $\overline{M} = 0.50$**

The corresponding adiabatic effectiveness contours are shown in Fig. 13. Because the surface is modeled as adiabatic, the surface temperature of the CFD model directly follows the adiabatic wall temperature, a fluid property, rather than some damped temperature that would occur on an actual conducting component. In Fig. 13 the region of nonzero $\eta$ at $T = 3.4$ is due to seepage of coolant out of the hole (also see $T = 3.4$ in Fig. 12) as a result of continuous mixing between the fluid in the coolant hole and the external flow during the period that the coolant is off. After the coolant jet is turned on ($T = 3.4$ through $T = 3.8$), the momentum of the jet increases and the region of elevated $\eta$ moves to the lower end of the coolant hole. As this occurs, the region of elevated $\eta$ from the coolant seepage during the off-period shrinks until it disappears at $T = 3.7$. The adiabatic effectiveness in that region is actually higher while the coolant jet is off than while the coolant jet is on.

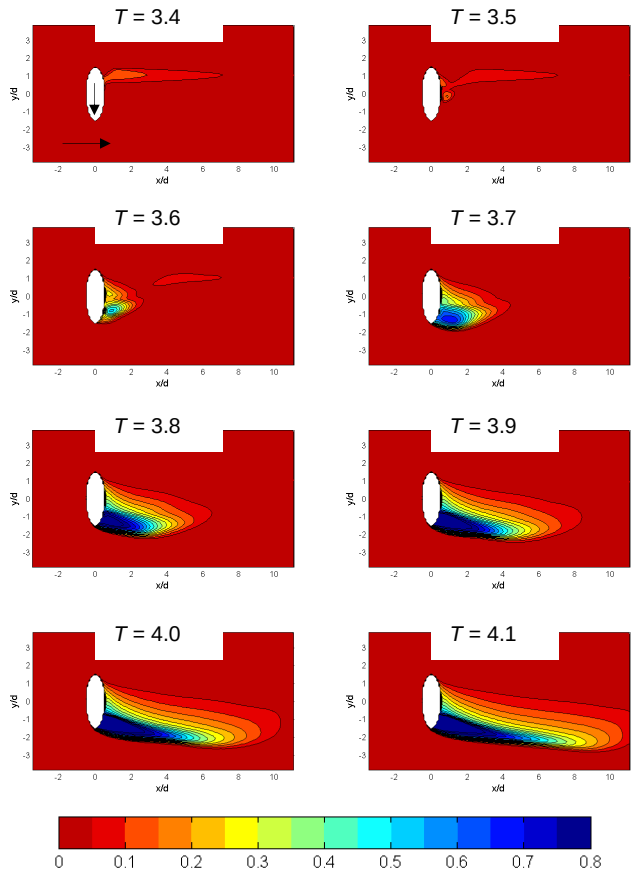


**Fig. 13 Adiabatic effectiveness contours for transient jet startup for the case of pulsed coolant between $M$ = 1 and $M$ = 0, $\overline{M}$ = 0.50 (arrows indicate direction of coolant and freestream)**

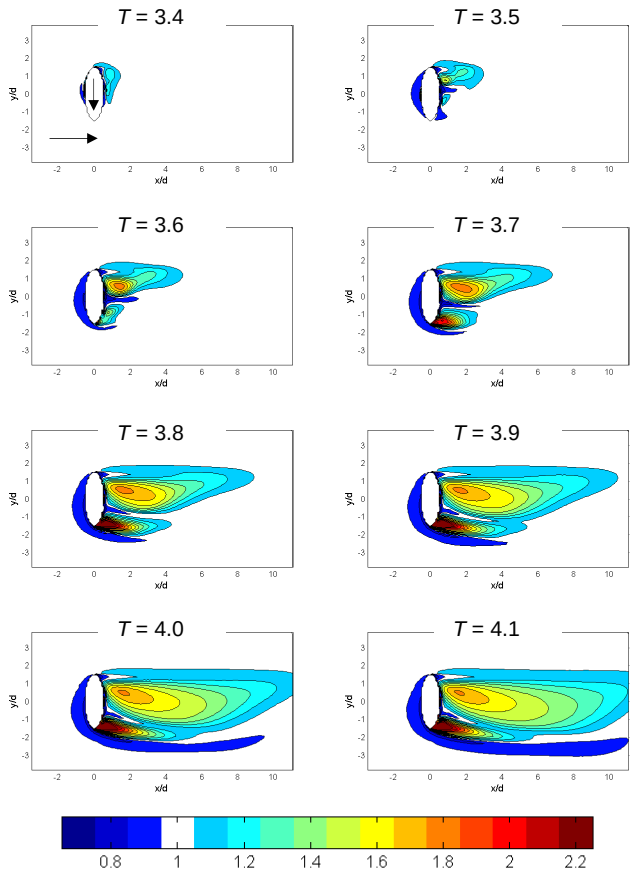


**Fig. 14 $h_f/h_0$ contours for transient jet startup for the case of pulsed coolant between $M$ = 1 and $M$ = 0, $\overline{M}$ = 0.50 (arrows indicate direction of coolant and freestream)**

Heat transfer coefficient ratio, $h_f / h_0$, contours for the transient startup event for the pulsed case between $M$ = 1 and $M$ = 0, are shown in Fig. 14. The heat transfer coefficient generally increases during the course of the transient event. Immediately evident by comparing $h_f / h_0$ in Fig. 14 to $\eta$ in Fig. 13 at $T$ = 4.1, which is nearing steady state condition, is that of the two tines of elevated $h_f / h_0$, the more severe one is protected by the highest levels of adiabatic effectiveness; however, the region of the top tine has much less protection from the film coolant.

With temporally resolved heat transfer coefficient distributions and adiabatic effectiveness data, we can compute the average net heat flux reduction, shown in Fig. 15. As one might expect from Figs. 13 and 14, there is a large region of negative net heat flux reduction (thus it is a region of net heat flux increase) where the heat transfer coefficient is elevated by the jet without a commensurate increase in adiabatic effectiveness. In this region the net heat flux is increased 20%. However, downstream of the lower part of the coolant hole, a favorable net heat flux reduction exists, with the 60% contour extending to $x/d$ = 5. The coolant seepage from the top of the coolant hole during the time that the coolant jet is off results in an elevated $\overline{\Delta q_r}$ downstream of the top of the coolant hole.

The role of the cross coupling term alone in influencing the net heat flux reduction is shown in Fig. 16. The region in which this term accounts for an effect greater than 5% is narrow, but extends to $x/d$ = 4. Immediately adjacent to the coolant hole, the term accounts for a 50% net heat flux reduction. It is also important to note that this term has a

beneficial effect wherever $h_f$ and $\eta$ fluctuate in phase, as is generally the case. Although not shown, the erroneous average net heat flux reduction that would have been obtained by improperly substituting $\overline{h_f}$ and $\overline{\eta}$ into Eq. (3) would be given by the difference of the values reported in Figs. 15 and 16.

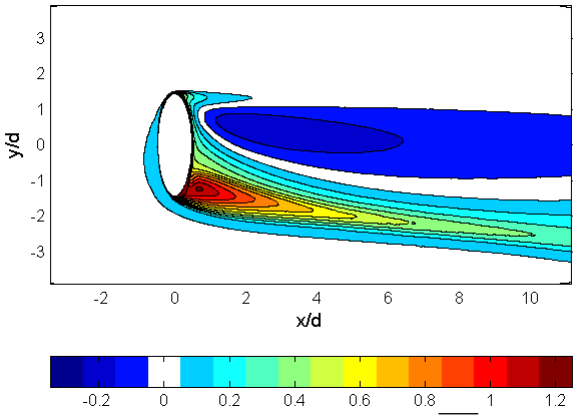


**Fig. 15 Average net heat flux reduction, $\overline{\Delta q_r}$, for the case of pulsed coolant between $M$ = 1 and $M$ = 0, $\overline{M}$ = 0.50, $\overline{M}$ = 0.50**

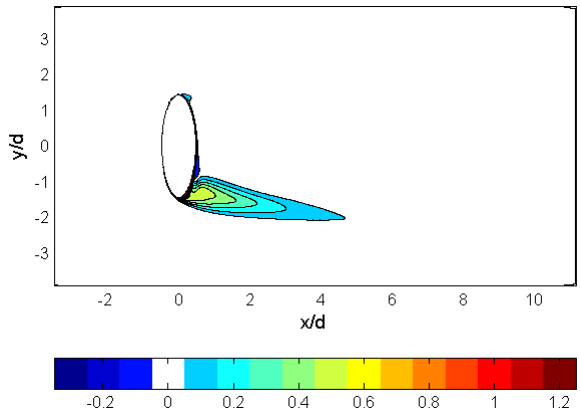


**Fig. 16 Influence of cross coupling term alone, $\overline{h_f'\eta'}/(h_0\phi)$, on average net heat flux reduction for the case of pulsed coolant between $M$ = 1 and $M$ = 0, $\overline{M}$ = 0.50**

In addition to the case of coolant pulsed between $M$ = 1 and $M$ = 0, the case of pulsed between $M$ = 0.75 and $M$ = 0.25 with the same average blowing ratio was also studied. Average net heat flux reduction is shown in Fig. 17. The region of negative net heat flux reduction downstream of the top of the hole is smaller than with the $M$ = 1 and $M$ = 0 case due to better film coverage afforded in that region during the period that the film coolant is at $M$ = 0.25.

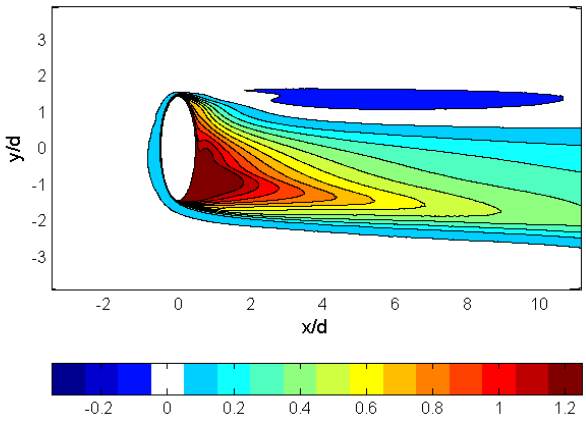


**Fig. 17 Average net heat flux reduction, $\overline{\Delta q_r}$, for the case of pulsed coolant between $M$ = 0.75 and $M$ = 0.25, $\overline{M}$ = 0.50**

Net heat flux reduction results for two pulsed cases with $\overline{M}$ = 0.25 are shown in Figs. 18 and 19. It is clear that neither case has net heat flux reduction superior to the steady jet case at the same average blowing ratio as shown in Fig. 9. As with the case of coolant pulsed between $M$ = 1 and $M$ = 0, a small region of elevated $\overline{\Delta q_r}$ is evident downstream of the top of the coolant hole due to coolant seepage during the $M$ = 0 period.

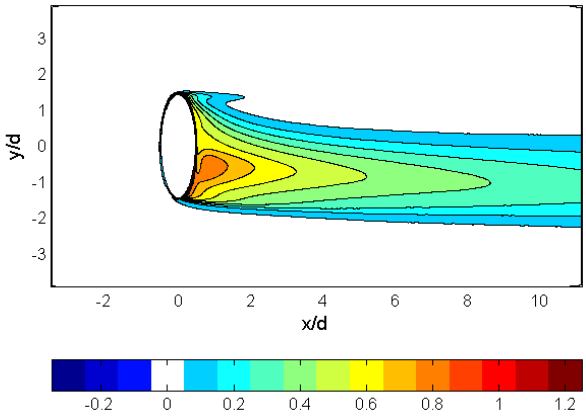


**Fig. 18 Average net heat flux reduction, $\overline{\Delta q_r}$, for the case of pulsed coolant between $M$ = 0.5 and $M$ = 0, $\overline{M}$ = 0.25**

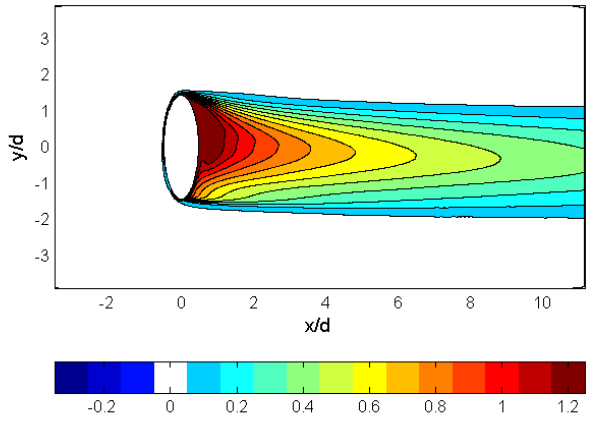


**Fig. 19 Average net heat flux reduction, $\overline{\Delta q_r}$, for the case of pulsed coolant between $M$ = 0.35 and $M$ = 0.15, $\overline{M}$ = 0.25**

In order to more generally characterize the performance of the various cooling schemes, adiabatic effectiveness results were spanwise averaged and plotted in Fig. 20. The region of spanwise averaging was taken to be $-3.93 < y/d < 3.93$, typical of the spacing between coolant holes on an actual blade. An improvement in adiabatic effectiveness by pulsing the coolant flow suggested by Ekkad et al. [2] is not evident in these results. For each average blowing ratio, the higher oscillation amplitudes yielded lower spanwise averaged adiabatic effectiveness. Although the computational geometry matches that of Ekkad et al. [2], the perfect square wave pulsation used in this computational study is impossible to achieve in the laboratory, and the precise waveform from the laboratory experiment is unknown. In particular, the capacitive effect of the plenum located between the valve and the hole, which was not modeled in the current computational study, could influence the waveform.

Simple spanwise averaging of the net heat flux reduction data would yield an average of a percent change. Instead, we seek a more useful indication of the reduction in the average heat flux along the spanwise direction defined as:

$$\Delta q_{r,span} = 1 - \frac{\int_{-\Delta y}^{\Delta y} q_f dy}{\int_{-\Delta y}^{\Delta y} q_0 dy} \qquad (7)$$

With unsteady film cooling, Eq. (7) becomes,

$$\overline{\Delta q_{r,span}} = 1 - \frac{\int_{-\Delta y}^{\Delta y} \left( \overline{h_f} \left( \phi - \overline{\eta} \right) - \overline{h_f' \eta'} \right) dy}{\int_{-\Delta y}^{\Delta y} h_0 \phi dy} \qquad (8)$$

The net heat flux reduction reported in this fashion is shown in Fig. 21. For the cases presented here, pulsing degrades performance with the severity of degradation being directly related to the amplitude in $M$. Because performance of steady film cooling with respect to blowing ratio in terms of the net heat flux reduction is peaked in nature with an optimum blowing ratio, alternating between two blowing ratios at a low frequency such that steady state arises during the cycle gives poorer performance than with steady coolant at the average blowing ratio.

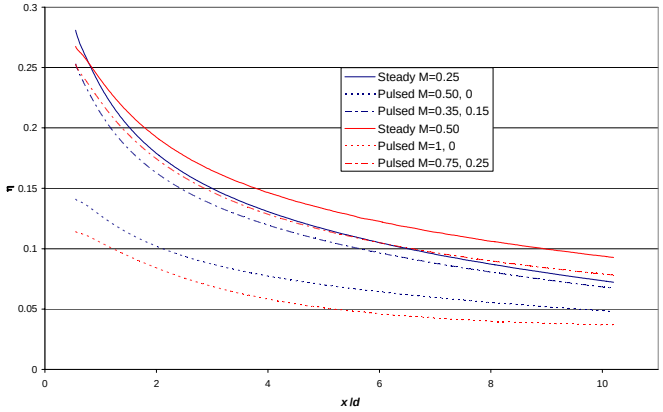


**Fig. 20 Spanwise averaged $\overline{\eta}$; $M$ = *A*, *B* indicates pulsing between $M$ = *A* and $M$ = *B***

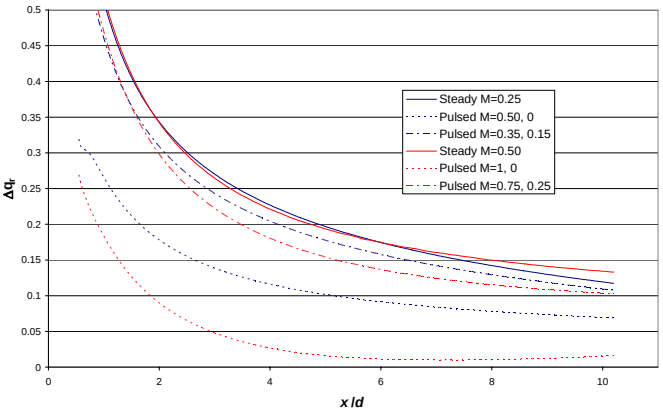


**Fig. 21 Net spanwise heat flux reduction $\overline{\Delta q_{r,span}}$; $M$ = *A*, *B* indicates pulsing between $M$ = *A* and $M$ = *B***

## CONCLUSION

The steady $M = 0.25$ and $M = 0.50$ cases both performed comparably in terms of net heat flux reduction. Although the $M = 0.50$ case had slightly higher spanwise averaged adiabatic effectiveness ($\Delta\eta \approx 0.02$) than the $M = 0.25$ case, the greater heat transfer coefficient resulted in very similar net heat flux reduction performance.

The cross coupled term in the unsteady form of the net heat flux reduction equation was demonstrated to have a 50% effect on net heat flux adjacent to the hole with decreasing

importance out to $x/d = 4.5$ for the case of coolant pulsed between $M = 1$ and $M = 0$. Although the term is of less importance for lower pulsation amplitudes, neglecting this term could lead to very large errors in $\overline{\Delta q_r}$. Because $h$ and $\eta$ tend to fluctuate in phase, the positive nature of the term would cause an analysis neglecting it to underestimate the net heat flux reduction.

Spatial and time resolved adiabatic effectiveness and heat transfer coefficient data demonstrate that net heat flux is generally increased by pulsing the film coolant at $F = 0.151$ and $DC = 50\%$. Heat transfer coefficient was only marginally affected by pulsing, with small reductions occurring particularly in cases for which the coolant is turned off during the cycle, evidently due to nonlinearity in the behavior of heat transfer coefficient with blowing ratio. The poorer net heat flux reduction performance of the pulsed schemes was rooted primarily in reduced adiabatic effectiveness, which in the more severe cases was cut in half by pulsing. The pulsing frequency is slow enough that transient events account for only approximately 30% of the total period, suggesting that the behavior of a pulsed scheme is dominated by the behavior of the average of behavior of the two blowing ratios between which the coolant fluctuates. The extent of this increase depends on the average blowing ratio and the amplitude of the oscillation, with poorer performance associated with greater oscillation amplitude.

*The views expressed in this article are those of the author and do not reflect the official policy or position of the United States Air Force , Department of Defense, or the U.S. Government.*

## REFERENCES


[1] Rutledge, J.L., King, P.I., Rivir, R., "Net Heat Flux Reduction for Unsteady Film Cooling," *Journal of Propulsion and Power* (submitted for publication).

[2] Ekkad, S. V., Ou, S., Rivir, R. B., "Effect of Jet Pulsation and Duty Cycle on Film Cooling From a Single Jet on a Leading Edge Model," *Journal of Turbomachinery*, Vol. 128, Jul., 2006, pp. 564-571.

[3] Coulthard, S., Volino, R., Flack, K., "Effect of Jet Pulsing on Film Cooling- Part I: Effectiveness and Flow-Field Temperature Results," *Journal of Turbomachinery*, Vol. 129, Apr., 2007, pp. 232-246.

[4] Coulthard, S., Volino, R., Flack, K., "Effect of Jet Pulsing on Film Cooling- Part II: Heat Transfer Results," *Journal of Turbomachinery*, Vol. 129, Apr., 2007, pp. 247-257.

[5] Muldoon, F. and Acharya, S., "Computations of Pulsed Film-Cooling," ASME Paper No. GT2007-28156, May 2007.

[6] Leylek, J. H. and Zerkle, R. D., "Discrete-Jet Film Cooling: A Comparison of Computational Results with Experiments," *Journal of Turbomachinery*, Vol. 116, 1994, pp. 358-368.

[7] Pointwise, Inc., *Gridgen Version 15 User's Guide*, Fort Worth, Texas, 2006.

[8] Marcum, D. L., "Advancing-Front/Local-Reconnection (AFLR) Unstructured Grid Generation," *Computational Fluid Dynamics Review*, 1998.

[9] Fluent Inc., *Fluent User's Guide*, Release 6.2, Lebanon, New Hampshire, 2005.

[10] Harrison, K. and Bogard, D., "CFD Predictions of Film Cooling Adiabatic Effectiveness for Cylindrical Holes Embedded in Narrow and Wide Transverse Trenches," ASME Paper No. GT2007-28005, May, 2007.

[11] Sen, B., Schmidt, D. L., and Bogard, D. G. "Film Cooling with Compound Angle Holes: Heat Transfer," *Journal of Turbomachinery*, Vol. 118, No. 4, pp. 800-806, 1996.

[12] Roland, I., "An Experimental Investigation of the Effect of Dimples on Turbine Adiabatic Film Cooling," M.S. Thesis, Air Force Institute of Technology, Mar., 2008.